Detecting Subsolar-Mass Primordial Black Holes in Extreme Mass-Ratio Inspirals with LISA and Einstein Telescope

Susanna Barsanti[,1,2,*] Valerio De Luca[,3,1,†] Andrea Maselli[,4,5,‡] and Paolo Pani[1,2,§]

¹*Dipartimento di Fisica, Sapienza Università di Roma, Piazzale Aldo Moro 5, 00185 Roma, Italy*
²*INFN, Sezione di Roma, Piazzale Aldo Moro 2, 00185 Roma, Italy*
³*Département de Physique Théorique and Centre for Astroparticle Physics (CAP), Université de Genève,*
24 quai E. Ansermet, CH-1211 Geneva, Switzerland
⁴*Gran Sasso Science Institute (GSSI), I-67100 L'Aquila, Italy*
⁵*INFN, Laboratori Nazionali del Gran Sasso, I-67100 Assergi, Italy*

Primordial black holes possibly formed in the early Universe could provide a significant fraction of the dark matter and would be unique probes of inflation. A smoking gun for their discovery would be the detection of a subsolar mass compact object. We argue that extreme mass-ratio inspirals will be ideal to search for subsolar-mass black holes not only with LISA but also with third-generation ground-based detectors such as Cosmic Explorer and the Einstein Telescope. These sources can provide unparalleled measurements of the mass of the secondary object at a subpercent level for primordial black holes as light as $\mathcal{O}(0.01)\ M_\odot$ up to luminosity distances around hundred megaparsec and few gigaparsec for LISA and Einstein Telescope, respectively, in a complementary frequency range. This would allow claiming, with very high statistical confidence, the detection of a subsolar-mass black hole, which would also provide a novel (and currently undetectable) family of sources for third-generation detectors.

Introduction.—Primordial black holes (PBHs) were proposed more than 50 yr ago [1–4] as BHs possibly formed across a vast mass range during the radiation-dominated era from the collapse of very large inhomogeneities [5–8]. Besides being unique messengers for inflation, in certain mass ranges PBHs could comprise the entirety of the dark matter, and could seed supermassive BHs at high redshift [9–11]. For these reasons, a robust PBH detection would have dramatic consequences for astrophysics, cosmology, gravitation, and particle physics.

However, detecting PBHs has proved to be extremely challenging. On the one hand, various constraints exist for the fraction of PBHs in dark matter [12]. On the other hand, in certain allowed mass ranges it is hard to disentangle the effect of a PBH from the astrophysical foreground. A notable example are the BH mergers detected by current and future GW interferometers. In recent years, considerable effort has been made to understand whether (at least a fraction of) the GW events detected by LIGO-Virgo so far [13,14] are of primordial origin [15–33] (see Refs. [34,35] for reviews). While PBHs could explain the recently detected mass-gap events (GW190814 [36] and GW190521 [37]) and a subpopulation of PBHs is statistically preferred against certain astrophysical population models in the latest GW catalog [33], confidently claiming that a BH merger is of primordial origin is much more challenging. Attempts have been made for single-event detections using Bayesian model selection based on

astrophysically or primordial-motivated different priors [38], whereas catalog analyses could use the peculiar mass-spin-redshift distributions predicted for PBH binaries [21,26] or perform population studies [27–30,33]. Unfortunately, none of these strategies seem able to give irrefutable evidence due to uncertainties in both PBH and astrophysical models [33]. Future third-generation (3G) detectors such as Cosmic Explorer (CE) [39] and Einstein Telescope (ET) [40] could detect several PBH mergers at redshift $z > 30$, where astrophysical-origin mergers should not occur [30,41]. However, redshift measurements for those cosmological sources are typically inaccurate and prior dependent [42].

In this complex scenario, a promising road to disentangle PBHs from astrophysical ones would be detecting a subsolar-mass compact object, since astrophysical BHs are expected to be born with a mass larger than the Chandrasekhar one [43–46] (see Refs. [47–52] for constraints on subsolar objects from current GW data).

In this work, we argue that subsolar mass BHs can be identified with unparalleled statistical confidence level if they perform extreme mass-ratio inspirals (EMRIs) around a supermassive BH as those detectable by the future Laser Interferometer Space Antenna (LISA) [53] (see [54,55] for related studies), and also as EMRIs around intermediate-mass BHs which would provide a novel, currently undetectable, GW source for 3G ground-based detectors (see in particular Ref. [49] for bounds on the merger rate of binary
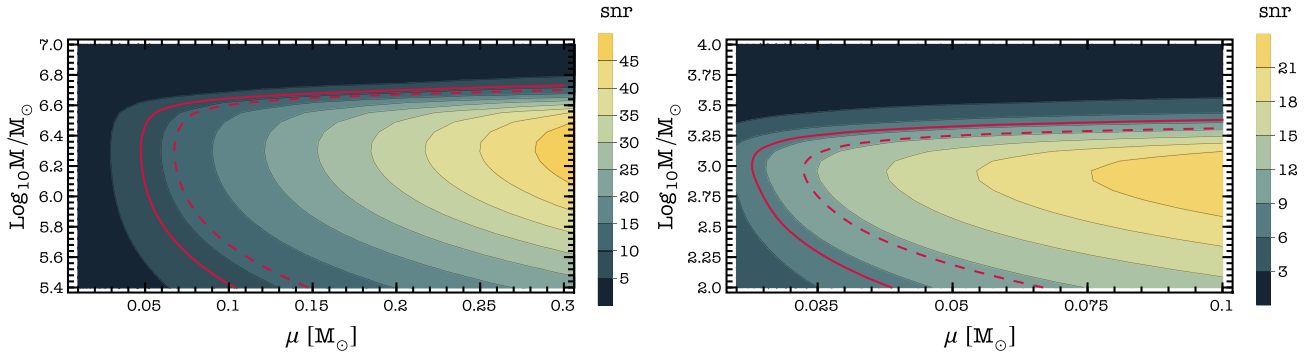
FIG. 1. SNR for EMRIs with primary mass M and subsolar secondary mass μ observed by LISA (left) and ET (right). In both cases we have fixed the primary spin to $\chi = 0.9$, assuming luminosity distance $d = 100$ Mpc ($d = 1$ Gpc) and signal duration $T = 1$ yr ($T = 1$h) for LISA (ET). The red solid (dashed) line identifies binaries with SNR = 8 (SNR = 11.3).

systems with large mass ratios and a subsolar mass component from the LIGO-Virgo data).

Setup.—Because of their tiny mass ratio $q = \mu/M \ll 1$, EMRI evolution can be modeled within BH perturbation theory [56,57], by studying the quasiadiabatic orbital motion of a point particle with mass μ (the secondary) around a much heavier BH with mass M (the primary). At variance with standard EMRI studies, we shall consider that the secondary is sufficiently lighter than a solar mass, $\mu < M_\odot$. We consider the leading-order adiabatic evolution, focusing on quasicircular, equatorial orbits around a Kerr BH and neglecting the spin of the secondary. The latter choice is motivated both because the spin of subsolar-mass PBHs is expected to be negligible [58–60], and because measurements of the other waveform parameters are not significantly affected by the secondary spin [61–65], the latter entering at first postadiabatic order.

We use the BH Perturbation Toolkit [66] to solve Teukolsky equation with arbitrary precision and compute the total energy flux $\dot{E}$ emitted by the binary. The adiabatic evolution of the inspiral is then driven by the emitted flux according to the evolution equations for the binary radius and phase

$$\frac{dr}{dt} = -\dot{E}\frac{dr}{dE_{\rm orb}}, \qquad \frac{d\Phi}{dt} = \frac{M^{1/2}}{r^{3/2} + \chi M^{3/2}}, \qquad (1)$$

where we focused on prograde orbits only, and $E_{\rm orb}$ denotes the binary orbital energy for a particle around a Kerr BH with mass M and dimensionless angular momentum χ [67]. The initial conditions (r_0, Φ_0) to integrate Eqs. (1) are chosen such that the secondary reaches an orbit within a distance, $r_{\rm plunge}$, of $0.1M$ from the innermost stable circular orbit (ISCO) in a given observation time T.

We then compute the corresponding GW signal using the quadrupole approximation [61,62], taking into account the detector pattern functions, which can be expressed in terms of the source orientation (θ_s, ϕ_s) and spin direction (θ_1, ϕ_1) in a solar barycentric frame, see Ref. [68] for ET and

Refs. [69,70] for LISA (henceforth we focus on ET; results with CE [39] would be qualitatively similar). We also take into account the phase modulation induced by the orbital motion [71], and an effective description of both the LISA and ET triangle configuration as a network of two L-shaped detectors, with the second detector rotated by 45° with respect to the first one.

The GW signal in the time domain is completely determined by the following set of parameters: $\vec{\theta} = (\ln M, \ln \mu, \chi, \ln d, \theta_s, \phi_s, \theta_1, \phi_1, r_0, \Phi_0)$, where d is the luminosity distance of the source. The corresponding signal-to-noise ratio (SNR) can be computed from the GW strain h as SNR $= \langle h|h\rangle^{1/2}$, where we have defined the usual inner product as $\langle h_1|h_2\rangle = 4\mathrm{Re}\int_{f_{\min}}^{f_{\max}}[\tilde{h}_1(f)\tilde{h}_2^\star(f)/S_n(f)]df$, in terms of the detector spectral density S_n, taken from the analytical fit of Ref. [72] for LISA (also including the confusion noise from unresolved white-dwarf binaries) and from Ref. [40] for ET-D. For both detectors the minimum frequency is set by requiring the binary to spend a time T to span the frequency band up to $f_{\max}$ when the secondary reaches $r_{\rm plunge}$. We assume that EMRIs are observed for $T = 1$ yr and $T = 1$h by LISA and by ET, respectively.

In the limit of large SNR, the posterior distribution of the source parameters $\vec{\theta}$ can be approximated by a multivariate Gaussian distribution centered around the true values $\vec{\theta}$ of the waveform parameters, with covariance $\mathbf{\Sigma} = \mathbf{\Gamma}^{-1}$, where $\Gamma_{ij} = \langle(\partial h/\partial\theta_i)|(\partial h/\partial\theta_j)\rangle_{\theta=\hat{\theta}}$ is the Fisher information matrix. The statistical error on the ith parameter is then given by $\sigma_i = \Sigma_{ii}^{1/2}$. In the limit of large SNR, the errors (and the inverse SNR) scale linearly with the luminosity distance of the source.

Because of the long and computationally expensive waveforms generated numerically in the time domain, along with their derivatives, Fisher matrices for EMRIs are characterized by large condition numbers, resulting in the need of high-precision numerical methods to compute the statistical errors accurately [73]. To this aim we have
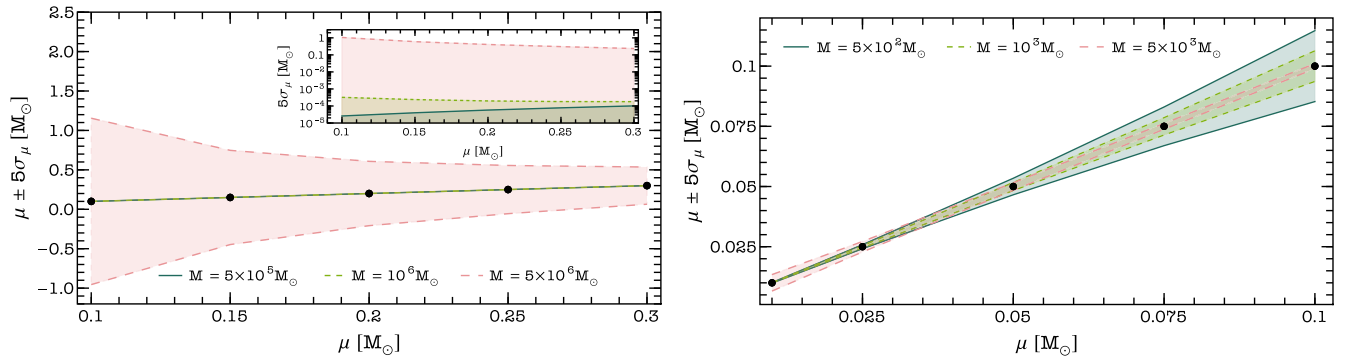
FIG. 2. Injected values of the secondary mass (black dots) and their 5σ interval inferred for EMRIs observed by LISA (left) and ET (right), assuming primary spin $\chi = 0.9$ and rescaling the distance such that SNR $= 8$. Color bands identify binaries with different values of the primary mass. In the left panel two of the bands are too narrow to be resolved; see inset for the 5σ (half) interval in logarithmic scale.

adopted the same setup discussed in [74]. In particular, we compute the exact GW fluxes and the Fisher matrix with high-precision numerics, which guarantees a stable evaluation of the covariance matrix.

Results.—We apply the numerical framework discussed above to investigate the detectability of EMRIs with a subsolar-mass secondary. In the left panel of Fig. 1 we show contour lines of fixed SNR for sources observed by LISA at $d = 100$ Mpc, as a function of their component masses, assuming the spin of the primary $\chi = 0.9$. (Hereafter, we fix the source angles to $\theta_s = \phi_s = \pi/2$ and $\theta_l = \phi_l = \pi/4$, although we have also checked that random sampling their values does not significantly affect our numerical results.) For a given M the SNR decreases rapidly for smaller values μ, since SNR $\sim q^3$ in the EMRI limit. Assuming a detection threshold SNR $= 8$ we find that, for the parameter space under consideration, binaries as distant as ~ 500 Mpc can be detected by LISA. For $d = 100$ Mpc only secondary BHs heavier than $\sim 0.05 \, M_\odot$ can be potentially observed. However, EMRIs with $\mu \sim 0.1 \, M_\odot$ feature SNR > 8 for a broad range of primary masses and can reach SNR as high as SNR ≈ 40 for $M \approx 10^6 \, M_\odot$ and $\mu \approx 0.3 \, M_\odot$. Assuming a larger threshold SNR $= 11.3$, equal to the strength of a signal observed by two aligned detectors with SNR $= 8$, one could potentially observe masses larger than $\sim 0.1 \, M_\odot$ and reach distances as large as ~ 400 Mpc.

The corresponding analysis for ET is shown in the right panel of Fig. 1. Because of the different frequency band covered by ground-based interferometers, we focus here on intermediate-mass primaries with $M \in [10^2, 10^4] \, M_\odot$, and $\chi = 0.9$. Interestingly, ET's horizon for these sources is larger than LISA's horizon for their supermassive counterparts: in the right panel of Fig. 1 we set $d = 1$ Gpc. EMRIs in this peculiar mass range would represent a new class of astrophysical sources for 3G interferometers, that can be observed with SNRs larger than those obtained for LISA binaries. At $d \sim 100$ Mpc ET would detect EMRIs with a secondary as small as $\mu \sim 10^{-2} \, M_\odot$ with SNR $\gtrsim 20$ for

$M \lesssim 2.5 \times 10^3 \, M_\odot$. Our analysis also suggests that ET can observe subsolar mass BHs at cosmological distances: a typical system with $(M, \mu) = (10^3, 10^{-1}) \, M_\odot$ would be seen at the SNR threshold up to few gigaparsec. This remarkable horizon is a peculiarity of the superior sensitivity (especially at low frequency) of 3G detectors such as ET relative to LIGO-Virgo. For the same sources shown in Fig. 1, the SNR in LIGO is smaller approximately by a factor 10 to 100 depending on the primary mass and spin, so all sources are well below the detectability threshold.

Despite their relatively low SNR, EMRIs are unique sources since their long orbital evolution provides measurements of the source parameters with unprecedented accuracy. This has been studied in detail only for standard LISA EMRI sources with $\mu \gtrsim M_\odot$ [61,63,65,71,74–76]. Here, we extend those analyses to subsolar secondaries and to ET for the first time. Projected constraints on the subsolar secondary mass are shown in Fig. 2 for LISA (left panel) and ET (right panel) and different binary configurations, assuming $\chi = 0.9$ and a conservative value for the threshold SNR $= 8$ (larger thresholds will result in even smaller errors). Our results show that both ground and space interferometers are able to measure the mass of a subsolar secondary component with subpercent precision in a large region of the detectable parameter space. For LISA, all systems with $M \lesssim 10^6 \, M_\odot$ would provide an indisputable identification of a subsolar component with $\mu \sim 0.1 \, M_\odot$, with relative uncertainties well below 0.1%. This would allow to exclude $\mu \gtrsim M_\odot$ for these systems at more than 5σ confidence level.

As shown in the right panel of Fig. 2, this picture does not change qualitatively for the family of EMRIs that could be observed by ET. Overall, ET will allow us to constrain values of the secondary BH mass down to $10^{-2} \, M_\odot$ for a wide range of primary mass [$M \in (10^2, 10^4) \, M_\odot$], with relative errors σ_μ/μ clustering below 10% for $\mu \gtrsim 0.025 \, M_\odot$, which would again allow excluding $\mu \gtrsim M_\odot$ at more than 5σ level.

The particular trend displayed by the errors in both panels of Fig. 2 is due to the dependence of the initial frequency $f_{\min}$ in terms of μ. In particular, for large values of the primary mass, the initial frequency approaches the detector reach, while for smaller M, $f_{\min}$ grows as μ decreases for a given observing time T.

Discussion.—We showed that, if subsolar BHs exist and form binaries around intermediate-mass and supermassive BHs, both LISA and ET are able to detect their inspiral up to distances of a hundred megaparsec and a few gigaparsec, respectively, and to identify a subsolar secondary mass in these sources at more than 5σ confidence level.

An important question concerns whether a subsolar-mass detection, however robust, can be ascribed to some compact object other than a PBH. White dwarfs and neutron stars are formed with masses, respectively, above $\approx 0.2\,M_{\odot}$ [77] and $\approx M_{\odot}$ in standard astrophysical scenarios. Furthermore, the Roche radius for a secondary white dwarf is larger than the ISCO of the primary when $\mu \gtrsim 0.002(M/10^3\,M_{\odot})M_{\odot}$, implying that white dwarfs and less compact stars (such as brown dwarfs) with $\mu \approx 0.2\,M_{\odot}$ would be tidally disrupted before their plunge into a BH with $M \lesssim 10^5\,M_{\odot}$. A similar conclusion holds also for brown dwarfs [78], with characteristic masses $\approx 10^{-2}\,M_{\odot}$, which would be tidally disrupted before reaching the ISCO. Therefore, a confident measurement of μ well below the solar-mass scale would necessarily imply new exotic physics. Arguably, the most natural explanation for such a remarkable claim would be a population of subsolar PBHs which, given current microlensing constraints in that mass range [79], could account for as much as a few percent of the dark matter [12]. In certain particle-dark-matter scenarios solar-mass BHs can form out of neutron star transmutation [80,81], but lighter BHs can essentially be of primordial origin only (see, however, Ref. [82] for models in which subsolar BHs are born out of dark sector interactions). Another possibility could be a subsolar exotic compact object [83], for example a boson star [84], although also the latter should be compact enough not to be tidally disrupted. In any case, detecting an EMRI with $\mu \ll M_{\odot}$ would imply new groundbreaking physics and should be included in the science case for fundamental physics with LISA [85] and 3G GW detectors [86].

Given the impact that such a detection would have, our study should be extended in various directions. We have focused on a relatively conservative scenario in which the primary's spin is $\chi = 0.9$. A faster-spinning primary would result in larger SNR, improving the detectability horizon by a factor of a few for $\chi = 0.99$. Likewise, for $\chi = 0.8$ the SNR decreases by a factor of a few relative to $\chi = 0.9$, reducing the detectable parameter space. The errors on μ depend on χ less significantly.

Interestingly, not only would subsolar-mass BHs around intermediate ones provide a novel source for 3G detectors but—given their mass ratio $q \sim 10^{-5}$ in the relevant parameter space—they would also allow exploiting the whole technology currently under development for standard EMRIs detectable by LISA, in particular first- and second-order self-force calculations [57,87,88] and sophisticated parameter-estimation strategies to extract the EMRI signal from the whole LISA data stream [76,89,90]. Likewise, we have focused on circular equatorial orbits, but the estimated errors on the secondary mass for standard EMRIs are similar for eccentric and inclined orbits [61,62,75], so we expect a comparable accuracy for EMRIs with $\mu \ll M_{\odot}$. EMRI parameter estimation is a challenging and open problem [62,75,76,90], which requires developing accurate waveform models, performing expensive statistical analysis, and also taking into account that the EMRI events in LISA might overlap with glitches, data gaps [91], and with several louder simultaneous signals from supermassive BH coalescences and other sources [89,90,92]. Detecting subsolar-mass EMRIs with LISA would face the same challenges. In comparison, detecting primordial-origin EMRIs with 3G detectors should be less demanding, since the signal can be considerably shorter without compromising detectability and parameter estimation. We have focused on a single 3G detector, but a network of ET plus one or two CE would further improve the overall SNR and the measurement errors.

The possibility of detecting subsolar BHs with 3G detectors gives further motivation to develop accurate waveform models for intermediate mass-ratio inspirals (IMRIs), since for $\mu \sim 0.1\,M_{\odot}$ and $M \sim (10^2\text{–}10^3)M_{\odot}$ the mass ratio $q \sim 10^{-4} - 10^{-3}$ is in a range where finite-size effects are particularly relevant. In the IMRI regime a combination of numerical simulations, high-order post-Newtonian and self-force calculations, as well as effective one-body techniques, should be used for an accurate modeling and parameter estimation [57,93–97].

Another important question concerns the detection rates for subsolar BHs in EMRIs and IMRIs. Unfortunately, even the rates for ordinary EMRIs are rather uncertain [75,95] and very little is known about the case of a subsolar-mass secondary. By assuming that PBHs follow the dark-matter density distribution and by rescaling standard EMRI rates to subsolar masses, Ref. [54] estimated that LISA could detect such sources as long as the fraction of PBHs in dark matter is a few percent. However, this conclusion relies on some approximations that should be carefully investigated. The rates for subsolar BHs around intermediate-mass BHs are even more uncertain, since the population of inter-mediate-mass BHs is essentially unknown. However, the recent GW190521 event [98] shows that BHs with masses around and above hundred $M_{\odot}$ form at least as a result of previous mergers. From our analysis, a subsolar secondary with $\mu \sim$ few $\times 10^{-2}\,M_{\odot}$ around a primary with $M \sim$ few $\times 10^2\,M_{\odot}$ could be detected and confidently identified by ET up to a few gigaparsec, and a two-detector ET + CE

network would improve this horizon approximately by 60% and would enlarge the detectable parameter space.

Finally, inspiraling binaries with subsolar components would emit a stochastic GW background which could be detected by LISA [99] and 3G detectors [100]. Resolving a primordial source would break the degeneracy between the PBH mass and abundance in the slope of the stochastic signal [99], thus possibly unveiling the nature of the unresolved sources.

[*] susanna.barsanti@uniroma1.it

[†] valerio.deluca@unige.ch

[‡] andrea.maselli@gssi.it

[§] paolo.pani@uniroma1.it

[1] Y. B. Zel'dovich and I. D. Novikov, Sov. Astron. **10**, 602 (1967).
[2] S. W. Hawking, Nature (London) **248**, 30 (1974).
[3] G. F. Chapline, Nature (London) **253**, 251 (1975).
[4] B. J. Carr, Astrophys. J. **201**, 1 (1975).
[5] P. Ivanov, P. Naselsky, and I. Novikov, Phys. Rev. D **50**, 7173 (1994).
[6] J. Garcia-Bellido, A. D. Linde, and D. Wands, Phys. Rev. D **54**, 6040 (1996).
[7] P. Ivanov, Phys. Rev. D **57**, 7145 (1998).
[8] S. Blinnikov, A. Dolgov, N. K. Porayko, and K. Postnov, J. Cosmol. Astropart. Phys. 11 (2016) 036.
[9] M. Volonteri, Astron. Astrophys. Rev. **18**, 279 (2010).
[10] S. Clesse and J. García-Bellido, Phys. Rev. D **92**, 023524 (2015).
[11] P. D. Serpico, V. Poulin, D. Inman, and K. Kohri, Phys. Rev. Research **2**, 023204 (2020).
[12] B. Carr, K. Kohri, Y. Sendouda, and J. Yokoyama, Rep. Prog. Phys. **84**, 116902 (2021).
[13] B. P. Abbott *et al.* (LIGO Scientific and Virgo Collaborations), Phys. Rev. X **9**, 031040 (2019).
[14] R. Abbott *et al.* (LIGO Scientific and Virgo Collaborations), Phys. Rev. X **11**, 021053 (2021).
[15] S. Bird, I. Cholis, J. B. Muñoz, Y. Ali-Haïmoud, M. Kamionkowski, E. D. Kovetz, A. Raccanelli, and A. G. Riess, Phys. Rev. Lett. **116**, 201301 (2016).
[16] M. Sasaki, T. Suyama, T. Tanaka, and S. Yokoyama, Phys. Rev. Lett. **117**, 061101 (2016); **121**, 059901(E) (2018).
[17] Y. N. Eroshenko, J. Phys. Conf. Ser. **1051**, 012010 (2018).
[18] S. Wang, Y.-F. Wang, Q.-G. Huang, and T. G. F. Li, Phys. Rev. Lett. **120**, 191102 (2018).
[19] Y. Ali-Haïmoud, E. D. Kovetz, and M. Kamionkowski, Phys. Rev. D **96**, 123523 (2017).
[20] Z.-C. Chen and Q.-G. Huang, Astrophys. J. **864**, 61 (2018).
[21] M. Raidal, C. Spethmann, V. Vaskonen, and H. Veermäe, J. Cosmol. Astropart. Phys. 02 (2019) 018.
[22] G. Hütsi, M. Raidal, and H. Veermäe, Phys. Rev. D **100**, 083016 (2019).
[23] V. Vaskonen and H. Veermäe, Phys. Rev. D **101**, 043015 (2020).
[24] A. D. Gow, C. T. Byrnes, A. Hall, and J. A. Peacock, J. Cosmol. Astropart. Phys. 01 (2020) 031.
[25] Y. Wu, Phys. Rev. D **101**, 083008 (2020).
[26] V. De Luca, G. Franciolini, P. Pani, and A. Riotto, J. Cosmol. Astropart. Phys. 06 (2020) 044.
[27] A. Hall, A. D. Gow, and C. T. Byrnes, Phys. Rev. D **102**, 123524 (2020).
[28] K. W. K. Wong, G. Franciolini, V. De Luca, V. Baibhav, E. Berti, P. Pani, and A. Riotto, Phys. Rev. D **103**, 023026 (2021).
[29] G. Hütsi, M. Raidal, V. Vaskonen, and H. Veermäe, J. Cosmol. Astropart. Phys. 03 (2021) 068.
[30] V. De Luca, G. Franciolini, P. Pani, and A. Riotto, J. Cosmol. Astropart. Phys. 05 (2021) 003.
[31] H. Deng, J. Cosmol. Astropart. Phys. 04 (2021) 058.
[32] R. Kimura, T. Suyama, M. Yamaguchi, and Y.-L. Zhang, J. Cosmol. Astropart. Phys. 04 (2021) 031.
[33] G. Franciolini, V. Baibhav, V. De Luca, K. K. Y. Ng, K. W. K. Wong, E. Berti, P. Pani, A. Riotto, and S. Vitale, arXiv:2105.03349.
[34] M. Sasaki, T. Suyama, T. Tanaka, and S. Yokoyama, Classical Quantum Gravity **35**, 063001 (2018).
[35] A. M. Green and B. J. Kavanagh, J. Phys. G **48**, 043001 (2021).
[36] S. Clesse and J. Garcia-Bellido, arXiv:2007.06481.
[37] V. De Luca, V. Desjacques, G. Franciolini, P. Pani, and A. Riotto, Phys. Rev. Lett. **126**, 051101 (2021).
[38] S. Bhagwat, V. De Luca, G. Franciolini, P. Pani, and A. Riotto, J. Cosmol. Astropart. Phys. 01 (2021) 037.
[39] D. Reitze *et al.*, Bull. Am. Astron. Soc. **51**, 035 (2019).
[40] S. Hild *et al.*, Classical Quantum Gravity **28**, 094013 (2011).
[41] S. M. Koushiappas and A. Loeb, Phys. Rev. Lett. **119**, 221104 (2017).
[42] K. K. Y. Ng, S. Chen, B. Goncharov, U. Dupletsa, S. Borhanian, M. Branchesi, J. Harms, M. Maggiore, B. S. Sathyaprakash, and S. Vitale, arXiv:2108.07276.
[43] A. L. Miller, S. Clesse, F. De Lillo, G. Bruno, A. Depasse, and A. Tanasijczuk, Phys. Dark Universe **32**, 100836 (2021).
[44] K. S. Phukon, G. Baltus, S. Caudill, S. Clesse, A. Depasse, M. Fays, H. Fong, S. J. Kapadia, R. Magee, and A. J. Tanasijczuk, arXiv:2105.11449.

[45] V. De Luca, G. Franciolini, P. Pani, and A. Riotto, J. Cosmol. Astropart. Phys. 11 (2021) 039.

[46] O. Pujolas, V. Vaskonen, and H. Veermäe, Phys. Rev. D **104**, 083521 (2021).

[47] B. P. Abbott *et al.* (LIGO Scientific and Virgo Collaborations), Phys. Rev. Lett. **121**, 231103 (2018).

[48] B. P. Abbott *et al.* (LIGO Scientific and Virgo Collaborations), Phys. Rev. Lett. **123**, 161102 (2019).

[49] A. H. Nitz and Y.-F. Wang, Phys. Rev. Lett. **126**, 021103 (2021).

[50] Y.-F. Wang and A. H. Nitz, Astrophys. J. **912**, 53 (2021).

[51] A. H. Nitz and Y.-F. Wang, Astrophys. J. **915**, 54 (2021).

[52] A. H. Nitz and Y.-F. Wang, Phys. Rev. Lett. **127**, 151101 (2021).

[53] P. Amaro-Seoane *et al.* (LISA Collaboration), arXiv:1702.00786.

[54] H.-K. Guo, J. Shu, and Y. Zhao, Phys. Rev. D **99**, 023001 (2019).

[55] F. Kuhnel, A. Matas, G. D. Starkman, and K. Freese, Eur. Phys. J. C **80**, 627 (2020).

[56] S. A. Teukolsky, Astrophys. J. **185**, 635 (1973).

[57] L. Barack and A. Pound, Rep. Prog. Phys. **82**, 016904 (2019).

[58] M. Mirbabayi, A. Gruzinov, and J. Noreña, J. Cosmol. Astropart. Phys. 03 (2020) 017.

[59] V. De Luca, V. Desjacques, G. Franciolini, A. Malhotra, and A. Riotto, J. Cosmol. Astropart. Phys. 05 (2019) 018.

[60] V. De Luca, G. Franciolini, P. Pani, and A. Riotto, J. Cosmol. Astropart. Phys. 04 (2020) 052.

[61] L. Barack and C. Cutler, Phys. Rev. D **69**, 082005 (2004).

[62] E. A. Huerta and J. R. Gair, Phys. Rev. D **84**, 064023 (2011).

[63] E. A. Huerta, J. R. Gair, and D. A. Brown, Phys. Rev. D **85**, 064023 (2012).

[64] G. A. Piovano, A. Maselli, and P. Pani, Phys. Rev. D **102**, 024041 (2020).

[65] G. A. Piovano, R. Brito, A. Maselli, and P. Pani, Phys. Rev. D **104**, 124019 (2021).

[66] Black Hole Perturbation Toolkit, http://bhptoolkit.org/.

[67] S. A. Hughes, Phys. Rev. D **61**, 084004 (2000); **63**, 049902 (E) (2001); **65**, 069902(E) (2002); **67**, 089901(E) (2003); **78**, 109902(E) (2008); **90**, 109904(E) (2014).

[68] R. Nair and T. Tanaka, J. Cosmol. Astropart. Phys. 08 (2018) 033; 11 (2018) E01.

[69] T. A. Apostolatos, C. Cutler, G. J. Sussman, and K. S. Thorne, Phys. Rev. D **49**, 6274 (1994).

[70] C. Cutler, Phys. Rev. D **57**, 7089 (1998).

[71] S. Babak, H. Fang, J. R. Gair, K. Glampedakis, and S. A. Hughes, Phys. Rev. D **75**, 024005 (2007); **77**, 04990(E) (2008).

[72] T. Robson, N. J. Cornish, and C. Liu, Classical Quantum Gravity **36**, 105011 (2019).

[73] J. R. Gair, M. Vallisneri, S. L. Larson, and J. G. Baker, Living Rev. Relativity **16**, 7 (2013).

[74] A. Maselli, N. Franchini, L. Gualtieri, T. P. Sotiriou, S. Barsanti, and P. Pani, Nat. Astron. (2021).

[75] S. Babak, J. Gair, A. Sesana, E. Barausse, C. F. Sopuerta, C. P. L. Berry, E. Berti, P. Amaro-Seoane, A. Petiteau, and A. Klein, Phys. Rev. D **95**, 103012 (2017).

[76] M. L. Katz, A. J. K. Chua, L. Speri, N. Warburton, and S. A. Hughes, Phys. Rev. D **104**, 064047 (2021).

[77] M. Kilic, C. Allende Prieto, W. R. Brown, and D. Koester, Astrophys. J. **660**, 1451 (2007).

[78] P. Amaro-Seoane, arXiv:2011.03059.

[79] P. Tisserand *et al.* (EROS-2 Collaboration), Astron. Astrophys. **469**, 387 (2007).

[80] B. Dasgupta, R. Laha, and A. Ray, Phys. Rev. Lett. **126**, 141105 (2021).

[81] P. Giffin, J. Lloyd, S. D. McDermott, and S. Profumo, arXiv:2105.06504.

[82] S. Shandera, D. Jeong, and H. S. G. Gebhardt, Phys. Rev. Lett. **120**, 241102 (2018).

[83] V. Cardoso and P. Pani, Living Rev. Relativity **22**, 4 (2019).

[84] H.-K. Guo, K. Sinha, and C. Sun, J. Cosmol. Astropart. Phys. 09 (2019) 032.

[85] E. Barausse *et al.*, Gen. Relativ. Gravit. **52**, 81 (2020).

[86] M. Maggiore *et al.*, J. Cosmol. Astropart. Phys. 03 (2020) 050.

[87] A. Pound, Phys. Rev. Lett. **109**, 051101 (2012).

[88] A. Pound, B. Wardell, N. Warburton, and J. Miller, Phys. Rev. Lett. **124**, 021101 (2020).

[89] LISA Data Challenge Working Group, LISA Data Challenges, 2019, https://lisa-ldc.lal.in2p3.fr.

[90] A. J. K. Chua, N. Korsakova, C. J. Moore, J. R. Gair, and S. Babak, Phys. Rev. D **101**, 044027 (2020).

[91] K. Dey, N. Karnesis, A. Toubiana, E. Barausse, N. Korsakova, Q. Baghi, and S. Basak, Phys. Rev. D **104**, 044035 (2021).

[92] P. Amaro-Seoane *et al.* (LISA Collaboration), arXiv:1702.00786.

[93] C. O. Lousto, H. Nakano, Y. Zlochower, and M. Campanelli, Phys. Rev. Lett. **104**, 211101 (2010).

[94] C. O. Lousto, H. Nakano, Y. Zlochower, and M. Campanelli, Phys. Rev. D **82**, 104057 (2010).

[95] P. Amaro-Seoane, Phys. Rev. D **98**, 063018 (2018).

[96] K. Jani, D. Shoemaker, and C. Cutler, Nat. Astron. **4**, 260 (2020).

[97] M. van de Meent and H. P. Pfeiffer, Phys. Rev. Lett. **125**, 181101 (2020).

[98] R. Abbott *et al.* (LIGO Scientific and Virgo Collaborations), Phys. Rev. Lett. **125**, 101102 (2020).

[99] Y.-F. Wang, Q.-G. Huang, T. G. F. Li, and S. Liao, Phys. Rev. D **101**, 063019 (2020).

[100] S. Mukherjee, M. S. P. Meinema, and J. Silk, Mon. Not. R. Astron. Soc. **510**, 6218 (2022).